

Molecular and atomic ultra trace analysis by laser induced fluorescence with OPO system and ICCD camera[☆]

L. Burel^a, P. Giamarchi^{a,*}, L. Stephan^a, Y. Lijour^b, A. Le Bihan^a

^a UMR-CNRS 6521, University of Bretagne Occidentale, 6 Av. Le Gorgeu, BP 809, 29285 Brest Cedex, France

^b Department of Chemistry, University of Bretagne Occidentale, 6 Av. Le Gorgeu, BP 809, 29285 Brest Cedex, France

Received 16 July 2002; received in revised form 9 October 2002; accepted 10 October 2002

Abstract

This paper presents a synthesis of some analytical potentialities of an equipment designed for both laser induced molecular and atomic fluorescence in the field of ultra-trace analysis (ng l^{-1}). Excitation of fluorescence was performed with a pulsed Nd:Yag laser coupled to an optical parametric oscillator (OPO). Fluorescence spectra were recorded with a spectrograph and an intensified charge-coupled device (ICCD). The high energy and the tunability of the excitation combined with the sensitivity of the ICCD and the time-resolution provide better limit of detection (LOD) and selectivity. By molecular fluorescence, some major organic contaminants in the environment were studied, i.e. polycyclic aromatic hydrocarbons (PAHs) (benzo[*a*]pyrene and hydroxypyrene) and a pesticide (carbaryl). The LODs achieved by direct analysis were far below the restricted European values for tap water. Analysis was performed in water containing humic acids using time resolution to avoid the matrix fluorescence. By electro thermal atomisation-laser excited atomic fluorescence (ETA-LEAF), we detected traces of aluminium and lead in seawater. Some general considerations about the signal to noise ratio optimisation are reported. LODs reached the femtogram level.

© 2003 Elsevier Science B.V. All rights reserved.

Keywords: Laser induced fluorescence; Laser with optical parametric oscillator (OPO) device; Ultra traces analysis; Poly aromatic hydrocarbons (PAHs); Pesticides; Aluminium; Lead

1. Introduction

Ultra-trace analysis of molecular and metal pollutants is a hard task because it generally requires extraction, concentration and separation

procedures which are time consuming. Moreover, it can induce contamination by reactants and loss of the analyte by adsorption type problems. To avoid these problems, analysis was performed by laser induced fluorescence (LIF) which is a very sensitive method [1,2] and permits a direct ultra-trace analysis. We built the experimental arrangement in the objective to make it suitable for both molecular and atomic fluorescence.

To increase LIF specificity, we used a pulsed Nd:YAG laser coupled with an optical parametric

[☆] Paper presented at the X International Symposium on Luminescence Spectrometry, Granada (Spain), 4–7 June 2002.

* Corresponding author.

E-mail address: phillippe.giamarchi@univ-brest.fr (P. Giamarchi).

oscillator (OPO) system [3,4] to tune the wavelength and an intensified charge-coupled device (ICCD) camera to record the time-resolved fluorescence spectra. Applications have been developed in direct ultra-traces analysis of molecular or metals pollutants in different matrix, like river-water or seawater. By molecular fluorescence, we studied polycyclic aromatic hydrocarbons (PAHs), hydroxypyrene and a carbamate pesticide. By atomic fluorescence, we studied aluminium and lead in seawater. More detailed protocols of some results recalled in this paper can be found in other specific articles for molecular fluorescence [5], and for atomic fluorescence [6].

PAHs are a family of naturally fluorescent organic pollutants [7]. They present a strong carcinogenic character and their total concentration is limited to $0.2 \mu\text{g l}^{-1}$ in drinking water [8] and $1 \mu\text{g l}^{-1}$ in raw water. The lower limits of detection (LODs) reached for benzo[a]pyrene by direct fluorescence methods are about 6–20 ng l^{-1} . They have been obtained by a diode laser fluorescence [9] or by synchronous fluorescence [10,11]. This paper reports the LODs obtained for the six PAHs normalised in Europe. A metabolite of PAHs, the hydroxy-pyrene, which can be found in contaminated animal or vegetal tissue is also studied.

At last, we paid attention to carbaryl, a naturally fluorescent carbamate pesticide, which is highly toxic to fish and birds [12]. It is used in cotton, fruits, nuts and other crops and is inherently toxic to humans by skin contact, inhalation and ingestion. In Europe, each pesticide is limited to $0.1 \mu\text{g l}^{-1}$ in tap water. The total pesticides are restricted to 0.5 or $5 \mu\text{g l}^{-1}$ for, respectively, tap and raw waters [8].

In these examples of natural matrix, like seawater or raw water, which present an important fluorescence signal, time-resolution is used to separate the analyte fluorescence signal from the matrix signal.

Electro-thermal atomisation laser excited atomic fluorescence (ETA-LEAF) is probably one of the most sensitive method for direct analysis of metal traces with a LOD in the range of 50 pg l^{-1} for lead or thallium for example [4,13]. As the electro-thermal atomisation atomic

absorption spectroscopy (ETA-AAS) ETA-LEAF presents the advantage to be usable for samples in a complex matrix as seawater or blood [14,15]. It is also a highly specific method because it combines the specificity of the neutral atom absorption and of their emission. However, for some important and complex matrices, some spectral interference may subsist. In this case, our set-up presents several advantages. First, the tunability and the high energy of the excitation, secondly the ICCD camera which allows us to obtain for the same impulsion the signal, the base line, and the possibility to detect an interference.

We first analysed aluminium in seawater because aluminium is a well-known anthropomorphic marker. Indeed, due to the complex seawater matrix, the usual atomic absorption methods are difficult and the lowest LOD by direct analysis reported in the literature is 30 ng l^{-1} [16]. We also studied lead in the same seawater matrix.

2. Materials and methods

Excitation of fluorescence is performed with a 10 Hz Nd:Yag laser coupled to an OPO and to a frequency doubler (continuum). The wavelength can be tuned from 225 to 1800 nm with a pulse width of 4–6 ns depending on the wavelength. The maximal pulse energy depends also on the wavelength with for example 30 mJ at 550 nm and 10 mJ at 275 nm.

The sample fluorescence is sent to a 750 mm focal spectrograph (Acton SP 750) and detected with an ICCD camera (ICCD Princeton Imax-512) Fig. 1. The intensifier of the ICCD had a minimum gate-time of 2 ns and the CCD chip had an active area of 512×512 pixels. A pulse-delay generator (Stanford Research System DG535) controlled the acquisition parameters (gate delay, gate width, and the gate step) of the CCD and allows to record time-resolved fluorescence spectra. The same experimental set up is used both for molecular and atomic fluorescence.

For molecular fluorescence, the beam excites the sample in a quartz cell and the energy was attenuated to about 1 mJ to avoid molecules

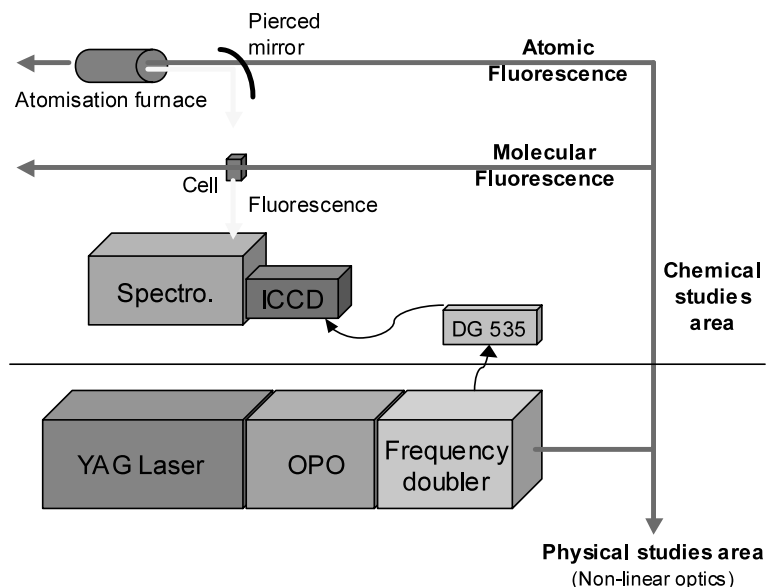


Fig. 1. Molecular and atomic fluorescence experimental set-up.

photobleaching. The 150 grooves mm^{-1} spectro-photograph grating is selected and a resolution of $0.2 \text{ nm pixel}^{-1}$ is obtained.

For atomic fluorescence, an additional set-up is used to send the laser beam to the centre of the graphite atomisation furnace (HGA 500 Perkin Elmer modified) through a pierced mirror. This mirror then collects the fluorescence emission of the sample and sends it to the spectrophotometer (Fig. 1). A 3600 grooves mm^{-1} grating is used to obtain the best resolution of 7 pm pixel^{-1} .

The set-up described combines the sensitivity of LIF and the excitation selectivity provided by the OPO system with the time resolution offered by the pulsed laser. This material has been purchased in collaboration with physicians researchers in a joint research program (LYOPO Program).

3. Molecular fluorescence experimental results

All the LODs are calculated using the IUPAC definition and with a standard deviation (S.D.) equal to three times blank σ . The λ values indicated for atomic fluorescence are issued from the NBS tables [17].

3.1. Poly aromatic hydrocarbons

Table 1 shows the LOD that we have been able to achieve in drinking water. These LOD are all below 10 ng l^{-1} and consequently always below the legal limits. For benzo[a]pyrene, we obtained a LOD of 0.7 ng l^{-1} in tap water, which is about ten times below the limit of 10 ng l^{-1} . In seawater, with the same experimental conditions, the LOD obtained is 1.65 ng l^{-1} . The linearity has been verified between 4 and 65 ng l^{-1} in tap water ($R^2 = 0.995$), and between 5 and 40 ng l^{-1} in seawater ($R^2 = 0.997$).

Table 1
Results obtained in drinking water for the six PAHs monitored in European Union and compared with the legal limit (total concentration of six PAHs $< 200 \text{ ng l}^{-1}$ and benzo[a]pyrene $< 10 \text{ ng l}^{-1}$)

PAHs	LOD (ng l^{-1})
Fluoranthene	10
Benzo[b]fluoranthene	1.8
Benzo[k]fluoranthene	5.5
Benzo[a]pyrene	0.7
Indeno[1,2,3-cd]pyrene	1.8
Benzo[ghi]perylene	6

The time-resolution benefits are important in the case of environmental samples like riverwater which contains an important fluorescent matrix responsible for an important noise. Fig. 2 shows the decrease of the benzo[*a*]pyrene signal at 400 nm versus the time delay. It is compared with the decrease of the humic acid solution noise computed on ten measurements. As the noise decreases faster than the signal, the use of a time-delay allowed elimination of the fluorescence matrix signal and increase of the signal-to-noise ratio. With a 45 ns delay, a detection limit of 4 ng l^{-1} for a 1 mg l^{-1} humic acid sample was obtained by direct analysis [5]. This result is far below the allowed limit of 1000 ng l^{-1} in raw water used for drinking water production. By comparison, without the delay, the LOD was only 25 ng l^{-1} .

3.2. Hydroxy-pyrene

We also studied hydroxy-pyrene which is one of the main metabolites of PAHs. Its LOD in water is 0.5 ng l^{-1} and the method linearity has been verified in a concentration range from 0 to 25 ng l^{-1} ($r^2 = 0.9974$).

Time-resolution allowed us to follow the decrease of the fluorescence signal with time. By extracting the data of the fluorescence intensity at 390 nm versus the time after the laser pulse, the decrease in fluorescence signal is shown in Fig. 3. By fitting this data with an exponential decay equation, we obtained a fluorescence lifetime of 15 ns in non-deoxygenated water.

In natural samples, hydroxy-pyrene can be found after marine pollution, for example in the liver of contaminated fish or in the cellular tissues of algae or halophytes plants.

We studied a salicornia (halophyte plant) extract in methanol. We used a time delay of 50 ns to reduce the matrix fluorescence because the salicornia extract has a shorter lifetime (7 ns) than the hydroxypyrene (30 ns). Fig. 4 shows the fluorescence spectrum of hydroxypyrene at 50 ng l^{-1} in a tissue extract of salicornia. One can see, middle curve, the spectrum of the salicornia extract in methanol; upper curve, the spectrum of the salicornia contaminated by hydroxy-pyrene and in lower curve the hydroxy-pyrene spectrum obtained by subtraction. The LOD obtained in this case is 30 ng l^{-1} . This type of analysis allows

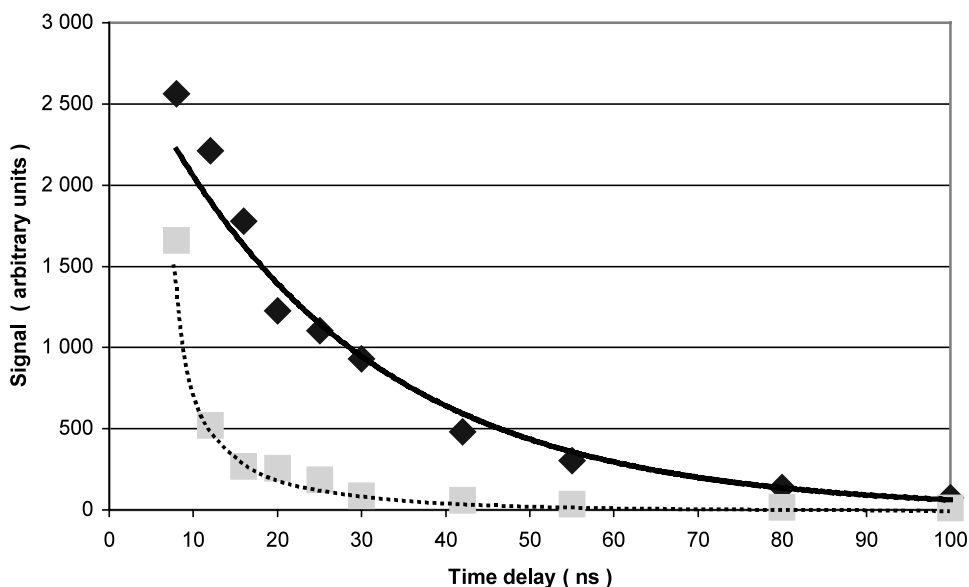


Fig. 2. Variation vs. the time delay of the benzo[*a*]pyrene signal (◆) with its exponential regression curve and of the humic acid solution noise computed on ten measurements (■). (with $\lambda_{\text{EX}} = 295 \text{ nm}$ and $\lambda_{\text{EM}} = 409 \text{ nm}$).

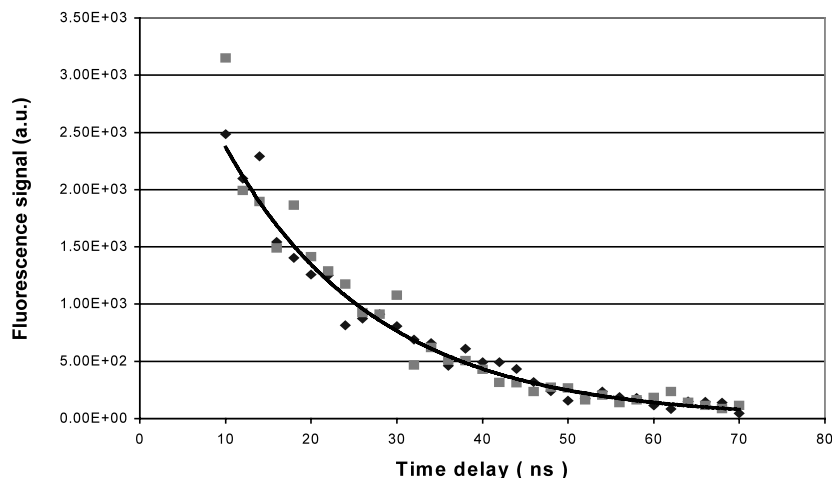


Fig. 3. Variation of the hydroxy-pyrene fluorescence signal vs. the time after the pulse laser. Two experimental series are plotted with an exponential fitting.

also monitoring low pollution levels in seawater and measurements of their long-term effects.

3.3. Carbaryl

We studied carbaryl as an example of pesticide that can be encountered in tap water accidental contamination. Fig. 5 shows the fluorescence of a 200 ng l^{-1} carbaryl solution in tap water. By exciting the sample at 277 nm , we were able to obtain a LOD of 20 ng l^{-1} and the linearity of the method was checked between 60 ng l^{-1} and $1.6 \mu\text{g l}^{-1}$. ($R^2 = 0.996$). A carbaryl fluorescence lifetime

of 27 ns was measured in non deoxygenated distilled water.

We attempt to detect carbaryl in a 1 mg l^{-1} humic acid solution. As the fluorescence lifetime of humic acids is short, we can use a time delay of 30 ns to avoid their strong fluorescence. By the way, a LOD of 30 ng l^{-1} was obtained for a fresh solution, in which carbaryl and humic acids were mixed just before the measurement. Further experiments were done after 30 min . The fluorescence of carbaryl was partially quenched because of the association of carbaryl with humic acids [18]. So, it should be keep in mind that only non-

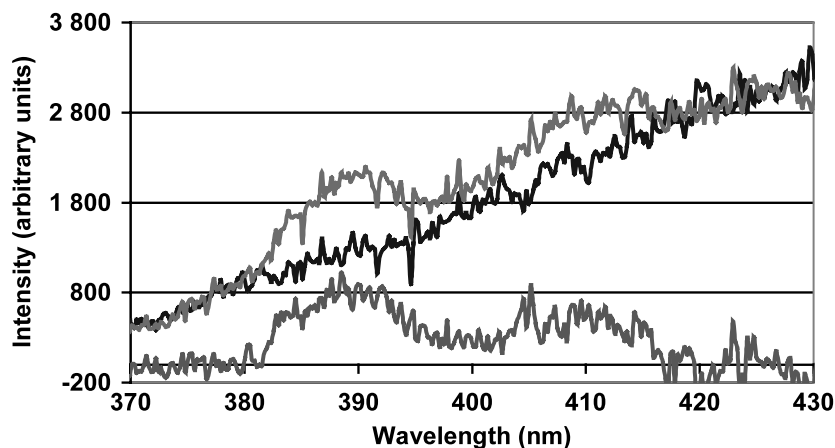


Fig. 4. Fluorescence spectrum of a tissue extract of: salicornia pure extract in methanol (middle curve); extract containing 50 ng l^{-1} of hydroxy-pyrene (upper curve); hydroxy-pyrene spectrum obtained by subtraction (lower curve).

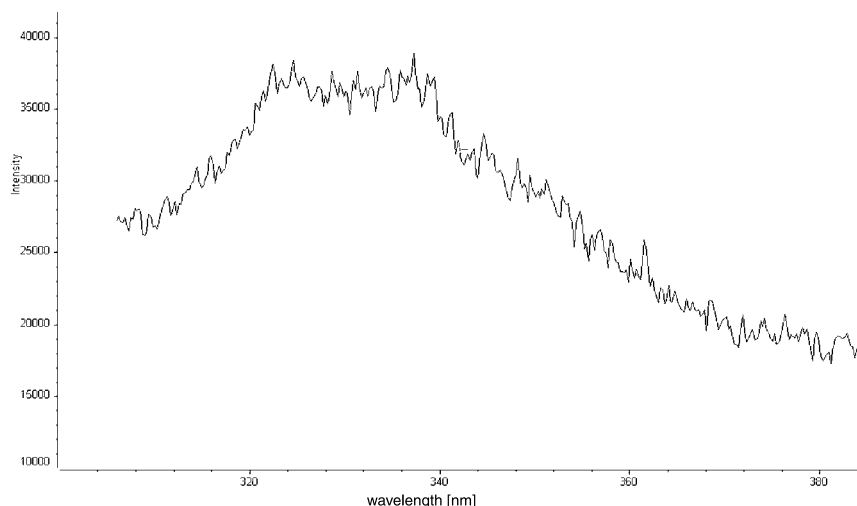


Fig. 5. Fluorescence spectrum of a 200 ng l⁻¹ carbaryl solution in drinking water.

associated carbaryl molecules are detected by direct fluorescence measurements on solutions containing humic acids.

4. Atomic fluorescence experimental results

In ETA-LEAF, volumes of samples atomised are low (generally inferior to 30 μ l), consequently a good optimisation of the signal to noise ratio is required to obtain the lowest LOD. As in ETA-AAS, it is necessary to optimise the furnace parameters (temperature, heating steps, gas flow, injected volume and modifier nature).

However, in ETA-LEAF, the signal intensity depends also on the excitation-emission wavelength pair, the pulse energy (until saturation of the atoms), the matrix pre-filter effect and the optical set-up performance. Consequently, to obtain the better LOD, numerous parameters have to be optimised.

Moreover, two important differences appear between the two methods on the noise and on the non specific absorption.

In ETA-AAS, the furnace temperature does not influence the noise, whereas in atomic fluorescence the thermal photons induce an important interference effect. At a given wavelength, the quantity of thermal photons increases with the temperature

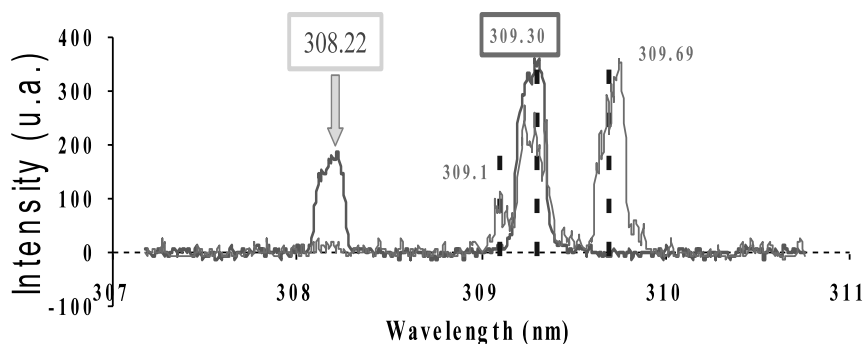


Fig. 6. Interference of magnesium fluorescence spectrum (thin line) with aluminium one (bold line).

(following the Planck law) and the noise is worsened (Fig. 7).

The noise results also from the camera reading noise, the others parasite photons (which are induced by the laser scattered light and the weak optics fluorescence). We have shown that the photons and the camera reading noises are non-Gaussian, but, despite of this, the total noise expressed by its $S.D._{TOT}$ and can be estimated with the classical formula:

$$s_{TOT}^2 = s_{Th}^2 + s_p^2 + s_{read}^2$$

where s_{Th} , s_p and s_{read} are, respectively, the thermal noise, the other parasite photons noise and the reading noise of the camera. It express that the atomisation temperature and the intensity of the laser shoot are important parameters of the method. At last, an other important point to reduce the noise is the optimisation, the time delay and the gate width.

In ETA-AAS with Zeeman or D_2 correction, the non specific absorption A_{BG} induces a signal to noise ratio decrease equal to $\sqrt{10^{ABG}}$; whereas in atomic fluorescence, the signal to noise ratio decreases by a factor 10^{ABG} because of the pre-filter effect.

As result of these two points, in ETA-LEAF, a low temperature atomisation in the presence of a low argon flow lower the noise and reduce the non specific absorption. Consequently, the LODs ob-

Table 2

Optimised experimental conditions for ETA-LEAF determinations in seawater

	Aluminium	Lead
$\lambda_{exc}/\lambda_{emission}$	257.509 nm/ 309.284 nm	283.305 nm/ 405.781 nm
Beam energy (μJ)	50	25
Time delay (ns)	5	3
Gate width (ns)	20	10
Injected volume (1% HNO_3 seawater) (μl)	20	10
Atomisation temperature ($^{\circ}C$)	2500	1700
Argon flow ($ml\ min^{-1}$)	0	10
ICCD amplification gain	200	200
Slit width (mm)	0.5	0.5

tained in these conditions are better than the classical ETA-AAS conditions, even if they increase the formation time of the neutral atoms [16]. For example, in the determination of lead in seawater (with optimised time-parameters and pulse energy), the use of an atomisation temperature of $1700\ ^{\circ}C$ instead of $2300\ ^{\circ}C$ and the use of $10\ ml\ min^{-1}$ argon flow instead of gas stop allowed to increase the signal to noise ratio by a factor three.

All the optimised parameters are presented in the Table 2 for both aluminium and lead determi-

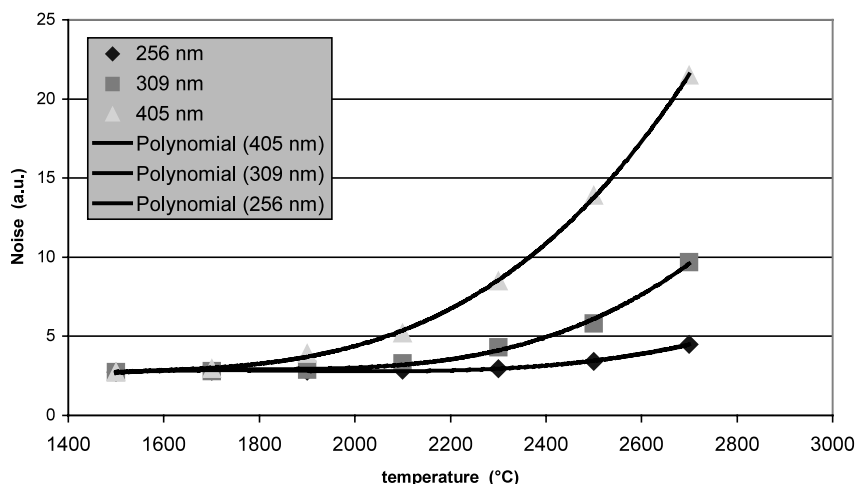


Fig. 7. Evolution of the thermal noise vs. the atomisation temperature.

nation in seawater. The LOD obtained in such experimental conditions, after addition of 1% nitric acid in seawater, are 5 ng l^{-1} for aluminium and 0.3 ng l^{-1} for lead.

We also showed that ICCD camera allows to highlight easily the spectral interference, like in Fig. 6, where the magnesium emission line at 309.30 nm interferes with aluminium. This interference occurs because of the high concentration of magnesium in seawater (approximately 0.05 mol l^{-1}). It can induce a significant error for low aluminium concentrations if the pulse energy is above to $75 \text{ }\mu\text{J}$. However, this interference becomes negligible by reducing the beam energy to $50 \text{ }\mu\text{J}$, which reduces the laser spectral wings, and by using a time delay of 5 ns.

5. Conclusion

These results demonstrate the capabilities of the 'LYOPO' system. Its sensitivity allows direct ultra-trace analysis of organic and metal pollutants, avoids consequently contamination by reactants and saves time by suppressing extraction procedures.

In molecular fluorescence, the use of time-resolution increases specificity by reducing the fluorescence matrix signal and consequently improves the signal-to-noise ratio and the LOD.

In atomic fluorescence, time-resolution reduces the noise induced by the laser scattered light and from the thermal photon, which consequently improves the signal to noise ratio and the detection limit. These two advantages compensate for the low laser frequency of 10 Hz which allows a limited number of measures during the atomisation.

As future developments, the research will focus first on improving the selectivity by developing multi-component determination in mixtures [19,20], using both the LIF excitation–emission matrix and the temporal resolution and employing data analysis techniques like principal components regression and partial least square.

Acknowledgements

The authors are grateful to the 'Conseil Régional de Bretagne', 'Conseil Général de Bretagne', 'Communauté Urbaine de Brest' and CNRS for their financial support.

References

- [1] T. Vo-Dinh, D. Eastwood, ASTM Publishers, STRI 1066, Philadelphia, PA, 1990.
- [2] C. Gooijer, A.J. Mank, *Anal. Chim. Acta* 400 (1999) 281–295.
- [3] Z.X. Zhou, X. Hou, K.X. Yang, S.J. Tsai, R.G. Michel, *Appl. Spectrosc.* 52 (1998) 176A–189A.
- [4] P. Stchur, K.X. Yang, X. Hou, T. Sun, R.G. Michel, *Spectrochim. Acta Part B* 56 (2001) 1565–1592.
- [5] P. Giamarchi, L. Burel, L. Stephan, Y. Lijour, A. Le Bihan, *Anal. Bioanal. Chem.* 374 (3) (2002) 490–497.
- [6] A. Le Bihan, Y. Lijour, P. Giamarchi, L. Burel, L. Stephan, Direct determination of aluminium in seawater by ETA-LEAF, *Spectrochim. Acta* 58 (1) (2003) 15–26.
- [7] R.G. Harvey, Cambridge University Press, Cambridge, 1991.
- [8] European Community Conceal Directive 80/778/CEE (15/7/1980).
- [9] P. Karlitschek, F. Lewitzka, U. Bünting, M. Niederkrüger, G. Marowsky, *Appl. Phys. B* 67 (1998) 497–504.
- [10] C.L. Stevenson, T. Vo-Dinh, *Anal. Chim. Acta* 303 (1995) 247–253.
- [11] J.S. Miller, *Anal. Chim. Acta* 388 (1995) 27–34.
- [12] EPA, Chemical information fact sheet for carbofuran, 25 June, 1984.
- [13] D.J. Butcher, R.L. Irwin, J. Takahashi, G. Su, G. Wei, R.G. Michel, *Appl. Spectrosc.* 44 (1990) 1521–1532.
- [14] A.I. Yuzefowsky, R.F. Lonardo, M. Wang, R.G. Michel, *J. Anal. Atom. Spectrom.* 9 (1994) 1195–1202.
- [15] E.P. Wagner, B.W. Smith, J.D. Winefordner, *Anal. Chem.* 68 (1996) 3199–3203.
- [16] S. Salomon, P. Giamarchi, A. Le Bihan, H. Becker-Rob, U. Heitmann, *Spectrochim. Acta Part B* 55 (2000) 1337–1350.
- [17] J.R. Fuhr, W.C. Martin, A. Musgrove, J. Sugar, W.L. Wiese (Eds.), NIST, Atomic Spectroscopic Database. Version 2.0 W.C.M. Data, NIST, internet : http://aeldata.phy.nist.gov/cgi-bin/AtData/lines_form.
- [18] A spectrofluorimetric study of the binding of carbofuran, carbaryl and aldicarb with dissolved matter. F. Fang, S. Kanan, H.H. Patterson, C.S. Cronan, *Anal. Chim. Acta* 373 (1998) 139–151.
- [19] P. Giamarchi, L. Stephan, S. Salomon, A. LeBihan, *J. Fluorescence* 10 (2000) 393–402.
- [20] J.L. Beltrán, R. Ferrer, J. Guiteras, *Anal. Chim. Acta* 737 (1998) 311–319.